Hydrothermal Synthesis, Thermal, and Magnetic Data on New Alkaline Vanadium Phosphate $M_y(VO)_{9+x}(PO_4)_{4x}(HPO_4)_{12-4x}$ with M = Cs^+ ($y = 5.29$, $x = 1$) and M = NH_4^+, Rb^+ ($y \sim 5$, $x \sim 1$)

E. Le Fur, B. de Villars, J. Tortelier, and J. Y. Pivan*

Laboratoire de Physicochimie, Ecole Nationale Supérieure de Chimie de Rennes, Campus de Beaulieu, Avenue du Général Leclerc, 35700 Rennes, France

Received April 27, 2000

Brownish platelet crystals of $M_y(VO)_{9+x}(PO_4)_{4x}(HPO_4)_{12-4x}$ (M = Cs^+, $NH_4^+$and Rb^+) were prepared hydrothermally. The structure of $Cs_{\sim 5}(VO)_{10}(PO_4)_4(HPO_4)_8$ was solved from single-crystal X-ray diffraction data in the centrosymmetric monoclinic space group *C*2/*c* (No. 15) $a = 21.1951(8)$ Å, $b = 12.2051(4)$ Å, $c = 20.6230(8)$ Å, $\beta = 109.742(2)°$, $Z = 4$ ($R_1(Fo) = 0.054$, $wR_2(Fo^2) = 0.123$). The structure of $Cs_{\sim 5}(VO)_{10}(PO_4)_4(HPO_4)_8$ is described and compared to that of $K_2(VO)_3(HPO_4)_4$ previously reported by Lii. For the three compounds, thermogravimetric data and susceptibility measurements were investigated and were found to be in agreement with the structural study.

Introduction

Since the vanadyl pyrophosphate $(VO)_2P_2O_7$ has been referred as the most efficient catalyst for the synthesis of maleïc anhydride from light hydrocarbons,[1] the VPOs crystal chemistry has been extensively revisited in recent years. Nowadays, most of the research teams agree that the large number of parameters into the heterogeneous reaction medium (pH, time, dilution, reaction temperature, chemical nature of precursors, etc.) make an exact control of the reaction pathway illusive in many cases. As pointed out by Amoros et al.,[2] in situ analyses during the hydrothermal processes are difficult to perform because of "the black box nature inherent in the hydrothermal reactor". Therefore, accurate and relevant data on the different chemical species that actually occur during the syntheses remain obscure. As a consequence, the mechanisms involved during hydrothermal syntheses are not well understood.[2] Nevertheless, trends are currently emerging which have led to a great variety of solids obtained in a reproducible way as clean products suitable for physical measurements. In the course of our investigations on the M−V−P−O systems, pure phases of $M_y(VO)_{9+x}(PO_4)_{4x}(HPO_4)_{12-4x}$ were isolated with M = Cs^+ ($y = 5.29$, $x = 1$) and M = NH_4^+, Rb^+ ($y \sim 5$, $x \sim 1$). The present paper deals with the synthesis, the thermal behavior and the magnetic properties of these $M_y(VO)_{9+x}(PO_4)_{4x}(HPO_4)_{12-4x}$ compounds. Additionally, the crystal structure of $Cs_{\sim 5}(VO)_{10}(PO_4)_4(HPO_4)_8$ is described and compared with $K_2(VO)_3(HPO_4)_4$.[3]

Experimental Section

Synthesis, X-ray Diffraction and SEM Studies. Mixtures of M_2CO_3 (∼ 0.50 g), V_2O_5 (∼ 0.154 g), Zn^0 (∼ 0.10 g), TEACl (∼1.0 g, TEACl = tetraethylammonium chloride) were added to 5 mL of a solution ∼8 M H_3PO_4 and sealed in a 23-ml Teflon lined acid digestion bomb (Parr Instruments). The reactor was heated at 200 °C under autogenous pressure for 2 days. After slowly cooling to room temperature, the reaction products were filtered off, rinsed with distilled water and dried in air into a furnace maintained at 100 °C for 24 h. Prior to subsequent analyses, the reaction products were checked by visual examination under the microscope and appeared as intergrown brownish hexagonal shaped single crystals without visible byproducts. These crystals were crushed to powder and analyzed by X-ray diffraction using λ Cu Kα = 1.54178 Å which resulted in new patterns. Though the diffractograms resembled to each other, the autoindexing procedure using DICVOL91 resulted in different unit-cells and symmetry.[4] The cæsium and rubidium compounds were found to be monoclinic ($a_M = 21.172(5)$ Å, $b_M = 12.269(3)$ Å, $c_M = 20.760(5)$ Å, $\beta = 109.93(2)°$ for Cs^+; $a_M = 20.97(3)$ Å, $b_M = 12.09(1)$ Å, $c_M = 20.41(3)$ Å, $\beta = 108.3(1)°$ for Rb^+), whereas the ammonium derivative was indexed on the basis of an hexagonal unit cell ($a_H = 12.108(2)$ Å, $c_H = 57.79(2)$ Å) with extinction conditions indicative of rhombohedral symmetry. The monoclinic and hexagonal cells were related through $\mathbf{a}_M = \mathbf{a}_H + 2.\mathbf{b}_H$, $\mathbf{b}_M = \mathbf{a}_H$ and $3.\mathbf{c}_M = -(\mathbf{a}_H + 2.\mathbf{b}_H + \mathbf{c}_H)$. Single crystals studies were performed at room temperature using Enraf-Nonius diffractometers with graphite monochromated Mo Kα radiation (λ = 0.71073 Å) that confirmed the results obtained from the X-ray powder diffraction analyses. A first intensity data set was collected using a classical CAD-4 diffractometer that resulted in a partial structure model ($R_1(F_o) \sim 22\%$). A supplementary intensity data collection was then planned using a Charge Coupled Device detector but statistical indicators (χ^2 values) calculated, using the COLLECT program,[5] indicated that the quality of the crystals was not suitable for accurate intensity data collection and a fortiori structure determination. Subsequent SEM photographs revealed that the crystals were "sandwich-like" polycrystals roughly piled up perpendicular to a pseudo "3-fold axis" (Figure 1). Accordingly, supplementary syntheses were undertaken to improve the quality of the crystals that were successful when introducing the vanadium precursor as VCl_3. The relative ratios M/V/P and the filling rate of the reactor were unchanged and the mixtures were heated at 160 °C for 8 days. Reproducibility was attained and

* Corresponding author e-mail: jean-yves.pivan@ensc-rennes.fr

(1) Centi, G.; Trifiro, F.; Ebrer, J. R.; Franchetti, V. M. *Chem. Rev.* **1988**, *88*, 55−80.
(2) Amorós, P.; Dolores Marcos, M.; Beltrán-Porter, A.; Beltrán-Porter, D. *Curr. Opinion Solid State Mater. Sci.* **1999**, *4*, 123−131 and references therein.
(3) Lii, K. H.; Tsai, H. H. *J. Solid State Chem.* **1991**, *91*, 331−338.
(4) Louër, D.; Boultif, M. *J. Appl. Cryst.* **1991**, *24*, 987−992.
(5) COLLECT, DENZO, SCALEPACK, SORTAV, Kappa CCD Program Package, Nonius BV, Delft, The Netherlands, **1998**.

10.1021/ic000464y CCC: $20.00
Published on Web 12/12/2000

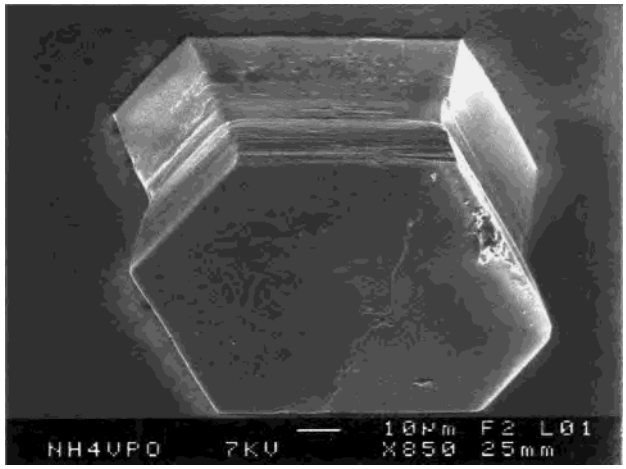

Figure 1. SEM photograph of a "sandwich-like" polycrystal of $(NH_4)_{\sim 5}(VO)_{10}(HPO_4)_8(PO_4)_4$.

Table 1. Crystal Data for $Cs_{\sim 5}(VO)_{10}(PO_4)_4(HPO_4)_8$

empirical formula	$Cs_{\sim 21}V_{40}P_{48}O_{232}H_{32}$
crystal system	monoclinic
space group	*C*2/*c* (n°15)
recording temperature	300 K
unit cell dimensions	$a = 21.1951(8)$ Å
	$b = 12.2051(4)$ Å
	$c = 20.6230(8)$ Å
	$\beta = 109.742(2)$
volume	$V = 5021.3(1)$ Å^3
Z	1
formula weight	10076.8 g.mol^{-1}
density (calc.)	3.33 g.cm^{-3}
absorption coefficient	60.7 cm^{-1}
residuals[a]	$R_1 = 0.0537$, $wR_2 = 0.1197$
goodness of fit	1.093
min., max. (e/Å^3)	−1.16, +1.51

[a] $R_1 = \sum||F_o| - |F_c||/\sum|F_o|$; $wR_2 = [\sum w(|F_o|^2 - |F_c|^2)/\sum w|F_o|^2]^{1/2}$ with $w = 1/[\sigma^2(F_o^2 + (0.0191P)^2 + 141.2619P]$; $P = (\max(F_o^2, 0) + 2F_c^2)/3$

very small single crystals were obtained especially in the case of the cæsium preparation. A well-shaped brownish platelet crystal of $Cs_{\sim 5}(VO)_{10}(PO_4)_4(HPO_4)_8$ was mounted on a glass fiber for intensity data collection using a CCD detector that revealed to be a powerful apparatus to enhance the number of recorded intensities though most of the diffracted spots were very weak. The COLLECT program was used to optimize the goniometer and detector angular settings during the intensity data collection that was conducted in the ω-ϕ scanning mode.[5] The unit cell and the orientation matrix were refined using the entire data set (17143 reflections) that was recorded up to $2\theta = 60°$. Reflection indexing resulted in a monoclinic unit-cell with parameters $a = 21.1951(8)$ Å, $b = 12.2051(4)$ Å, $c = 20.6230(8)$ Å, $\beta = 109.742(2)°$. 176 frames were collected for a total exposure of 286 min. Lorentz-polarization correction and peak integration were performed using the DENZO program and the data set was corrected using the SCALEPACK program.[5] Table 1 lists the crystallographic data and the reliability factors at the end of refinement. Examination of the intensity data revealed the systematic absences (hkl $h + l = 2n + 1$; $h0l$ $l = 2n + 1$) that were consistent with *Cc* (n°9) or *C*2/*c* (n°15) space groups. Direct methods were used to extract the starting structure model using SIR97,[6] and refinements were made against F_o^2 using SHELXL-97,[7] in the centrosymmetric space group *C*2/*c*. The entire structure model (non-hydrogen atoms) was obtained from successive difference Fourier maps. The hydrogen atoms were not located accurately and were input in the final formula according to accurate scrutiny of the framework counting the nonshared oxygen atoms on the phosphate groups. When refining the isotropic thermal factors, it was readily obvious that the Cs1, Cs2, Cs4, V6, and V7 sites were not fully occupied and that disorder might be present on the V2, V3, and V4 positions. So, the multiplicity for each metal atom was refined that resulted in Cs1 0.669(3); Cs2 0.632(3); Cs3 0.981(3); Cs4 0.308(2); V1 0.49(3); V2 0.46(2); V2′ 0.51(2); V3 0.54(2); V3′ 0.44(4); V4 0.46(2); V4′ 0.52(2); V5 0.95(1); V6 0.22(1); V7 0.24(1); P1 0.96(1); P2 0.93(1); P3 0.94(1); P4 0.98(1); P5 0.96(1); P6 0.97(1). At this stage of refinement, the reliability factors were $R_1(F_o) \sim 0.064$, $wR_2(F_o^2) \sim 0.157$ for 7341 unique reflections (4010 reflections with $I \geq 2\sigma(I)$) and 470 variable parameters. Careful examination of the result files from SHELXL-97 revealed very high reliability factors for the low $\lambda/\sin(\theta)$ values ($R_1(F_o) \geq 43\%$ for $\lambda/2.\sin(\theta) \leq 0.74$). Assumption was made that the numerous very weak intensities for the high θ values were not accurately estimated. Subsequent refinements were then run using a

Table 2. Positional Parameters and Equivalent Isotropic Displacement Parameters

atoms	*x*	*y*	*z*	sof	U_{eq} (Å^2)[a]
Cs1	0.90839(5)	0.41093(8)	0.96713(5)	0.679(3)	0.0267(4)
Cs2	0.75623(5)	0.58012(8)	0.02840(5)	0.643(3)	0.0287(4)
Cs3	0.05797(4)	0.07898(6)	0.43449(4)	1	0.0451(3)
Cs4	0.16779(10)	0.5829(2)	0.25272(10)	0.323(3)	0.0307(8)
V1	0.7500	0.2500	0.0000	1	0.0462(9)
V2	0.7830(3)	0.1635(5)	0.8341(2)	0.50	0.0131(11)
V2′	0.7899(3)	0.1664(5)	0.8630(2)	0.50	0.0116(11)
V3	0.0366(7)	0.5787(12)	0.3595(4)	0.50	0.014(2)
V3′	0.0292(7)	0.5749(12)	0.3373(3)	0.50	0.013(2)
V4	0.2254(5)	0.3380(9)	0.1616(3)	0.50	0.0100(14)
V4′	0.2141(5)	0.3331(9)	0.1381(3)	0.50	0.0128(15)
V5	0.91412(9)	0.25237(13)	0.50047(8)	1	0.0222(4)
V6	0.0000	0.9209(4)	0.2500	0.50	0.0241(10)
V7	0.0815(3)	0.1648(5)	0.2493(3)	0.25	0.0154(13)
P1	0.62828(12)	0.7061(2)	0.13706(12)	1	0.0159(5)
P2	0.93712(12)	0.3622(2)	0.36453(12)	1	0.0162(5)
P3	0.45035(12)	0.7074(2)	0.13168(12)	1	0.0168(5)
P4	0.72832(12)	0.4057(2)	0.13533(12)	1	0.0155(5)
P5	0.65117(12)	0.5906(2)	0.13046(12)	1	0.0161(5)
P6	0.14065(12)	0.3658(2)	0.36955(12)	1	0.0174(5)
O1	0.7232(4)	0.3709(5)	0.9338(3)	1	0.032(2)
O2	0.6716(4)	0.1631(6)	0.9461(3)	1	0.034(2)
O3	0.8021(3)	0.1837(5)	0.9480(3)	1	0.0226(15)
O4	0.6940(4)	0.4898(5)	0.1377(4)	1	0.031(2)
O5	0.3778(3)	0.6999(6)	0.8626(4)	1	0.033(2)
O6	0.7655(3)	0.1492(5)	0.7472(3)	1	0.0209(15)
O7	0.6930(3)	0.1310(6)	0.8349(3)	1	0.027(2)
O8	0.7672(4)	0.3219(5)	0.8384(3)	1	0.031(2)
O9	0.0000	0.5471(7)	0.2500	1	0.023(2)
O10	0.5659(3)	0.8793(6)	0.9466(3)	1	0.029(2)
O11	0.5902(4)	0.8088(6)	0.8331(4)	1	0.034(2)
O12	0.6069(4)	0.0240(6)	0.8632(4)	1	0.035(2)
O13	0.4615(4)	0.8175(5)	0.8395(3)	1	0.030(2)
O14	0.9780(4)	0.4647(6)	0.3698(4)	1	0.039(2)
O15	0.6672(3)	0.8108(5)	0.0517(3)	1	0.025(2)
O16	0.7616(4)	0.5156(5)	0.8718(4)	1	0.038(2)
O17	0.8636(3)	0.3928(6)	0.3407(4)	1	0.035(2)
O18	0.6958(4)	0.6857(5)	0.1637(3)	1	0.032(2)
O19	0.7008(3)	0.7179(6)	0.8675(4)	1	0.036(2)
O20	0.9585(3)	0.3028(6)	0.4341(3)	1	0.026(2)
O21	0.6248(4)	0.6803(5)	0.9344(3)	1	0.027(2)
O22	0.6113(4)	0.6106(5)	0.0538(3)	1	0.026(2)
O23	0.4945(3)	0.6926(5)	0.9439(3)	1	0.025(2)
O24	0.0000	0.0546(19)	0.2500	0.50	0.027(5)
O25	0.0162(13)	0.1031(21)	0.2478(15)	0.25	0.023(7)
OH1	0.5969(4)	0.6095(6)	0.8139(4)	1	0.036(2)
OH2	0.9502(5)	0.2861(6)	0.3105(4)	1	0.048(2)
OH3	0.4673(4)	0.6139(6)	0.8263(4)	1	0.040(2)
OH4	0.6565(4)	0.4166(7)	0.8117(4)	1	0.045(2)
OH5	0.5999(4)	0.5756(7)	0.1690(4)	1	0.041(2)
OH6	0.0883(4)	0.2762(6)	0.3356(4)	1	0.046(2)

[a] U_{eq} is defined as one-third of the trace of the orthogonalized U_{ij} tensor.

(6) Altomare, A.; Burla, M. C.; Camalli, M.; Cascarano, G. L.; Giacovazzo, C.; Guagliardi, A.; Moliterni, A. G. G.; Polidori, G.; Spagna, R. SIR97: a new tool for crystal structure determination and refinement. *J. Appl. Crystallogr.* **1999**, *32*, 115−119.

(7) Sheldrick, G. M.; SHELXL-97, Program for crystal structure refinement, University of Göttingen, Germany, **1997**.

Table 3. Selected Bond Lengths (Å) with Their Standard Deviation in Brackets for $Cs_{\sim 5}(VO)_{10}(PO_4)_4(HPO)_8$

V1	O3	1.956(6)	V2	V2′	0.566(4)	V2′	V2	0.566(4)
	O3	1.956(6)		O6	1.711(7)		O3	1.695(7)
	O1	1.959(6)		O5	1.944(9)		O5	1.911(9)
	O1	1.959(6)		O7	1.955(9)		O4	1.937(9)
	O2	1.969(7)		O8	1.969(9)		O8	1.981(9)
	O2	1.969(7)		O4	1.971(9)		O7	1.984(9)
				O3	2.258(7)		O6	2.276(7)
V3	V3′	0.432(4)	V3′	V3	0.432(4)	V4	V4′	0.466(4)
	O10	1.768(10)		O9	1.729(7)		O6	1.689(8)
	O14	1.92(2)		O11	1.94(2)		O18	1.967(12)
	O12	1.93(2)		O13	1.96(2)		O16	1.968(12)
	O13	1.97(2)		O12	1.96(2)		O19	1.974(12)
	O11	1.97(2)		O14	1.98(2)		O17	1.989(12)
	O9	2.160(7)		O10	2.194(10)		O15	2.209(9)
V4′	V4	0.466(4)	V5	O15	1.839(7)	V6	O24	1.63(2)
	O15	1.744(8)		O10	1.859(7)		OH3	1.967(7)
	O16	1.946(13)		O20	2.001(7)		OH3	1.967(7)
	O19	1.947(13)		O21	2.001(6)		OH1	2.064(7)
	O18	1.951(13)		O23	2.025(7)		OH1	2.064(7)
	O17	1.982(13)		O22	2.032(6)			
	O6	2.155(8)						
V7	O25	1.57(23)	P1	O11	1.504(7)	P2	O14	1.505(7)
	OH2	1.898(10)		O19	1.516(7)		O17	1.513(7)
	OH4	1.946(10)		O21	1.534(7)		O20	1.533(7)
	OH5	2.124(9)		OH1	1.550(7)		OH2	1.546(7)
	OH6	2.206(10)						
P3	O5	1.505(7)	P4	O16	1.499(7)	P5	O4	1.506(7)
	O13	1.520(7)		O8	1.523(7)		O18	1.508(7)
	O23	1.533(7)		O1	1.527(6)		O22	1.540(6)
	OH3	1.547(7)		OH4	1.551(7)		OH4	1.559(7)
P6	O12	1.509(7)						
	O7	1.509(7)						
	O2	1.531(7)						
	OH6	1.547(8)						

reduced data set up to $\theta = 25°$ that resulted in significant improvements of the agreement factors ($R_1(F_o) \sim 0.054$, $wR_2(F_o^2) \sim 0.123$ for 4430 unique reflections (3287 reflections with $I \geq 2\sigma(I)$), 453 variable parameters) and reasonable anisotropic displacement parameters for all atoms. In the last cycles, only the occupancy factors for the cæsium atoms were kept in refinement, those for vanadium V1 and V5 were fixed at 100%, those for V2, V3, V4, and V6 were fixed at 50%, for V7 at 25% and for phosphorus at 100%. Taking into account the relationships between the monoclinic and hexagonal cells, no conclusive structure solution was found in the possible supergroups $R\bar{3}m$ and $R\bar{3}c$ (the systematic absences $h\bar{h}0l$ with $l = 2n + 1$ were not fulfilled for the latter space group). Atomic positional coordinates and atomic displacement parameters are given in Table 2. Selected bond distances and angles are summarized in Table 3.

Structure Results and Discussion

The structure of $Cs_{\sim 5}(VO)_{10}(PO_4)_4(HPO_4)_8$ is shown in Figure 2 in projection along the [010] direction. It consists of distorted V-octahedra, square planar V-pyramids and regular P-tetrahedra that are polyhedra commonly found in the vanadium phosphates chemistry (see Figure 3). The vanadium octahedra share trans and cis vertices to form infinite ondulating chains that develop in the (010) plane. Along the chains, the trans and cis sharing occur in an ordered manner to form two different units: units of 5 trans sharing octahedra (unit 1) and units of 2 trans sharing octahedra (unit 2) which are linked together via a cis sharing distorted octahedron centered on V5 (Figure 4). The trans sharing octahedron around V1, located at the middle of unit 1, coupled with the cis sharing around V5 are the topological elements within the chain that remove the possibility for a 3_2 axis and a fortiori the possibility for the rhombohedral symmetry. The repeating sequence within the chain is 58.23 Å long. Units 1 and 2 have alternating short and long V−O bonds with

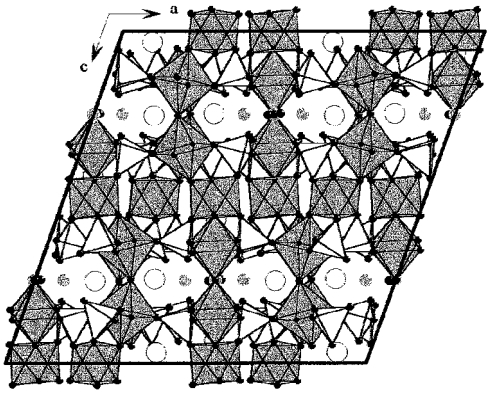

Figure 2. View of $Cs_{\sim 5}(VO)_{10}(HPO_4)_8(PO_4)_4$ along the [010] direction. Grey polyhedra are VO_6 octahedra, open ones are PO_4 tetrahedra. The V_3 trimers are not represented for sake of clarity. Grey circles inside the windows are the V6 and V7 ions involved in the trimers. Open circles are the Cs^+ cations. Black circles are oxygen atoms.

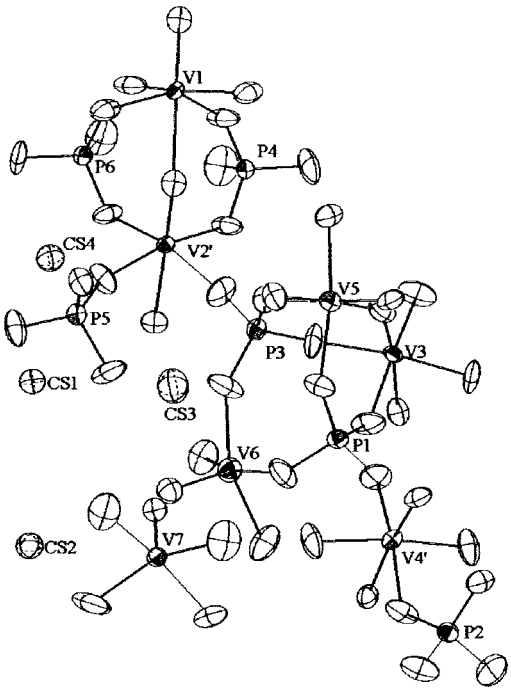

Figure 3. View of the asymmetric unit of $Cs_{\sim 5}(VO)_{10}(HPO_4)_8(PO_4)_4$ (ORTEP-style) showing the connectivity. Thermal ellipsoids are at the 70% probability level.

two types of V−O−V bond angles at the shared O atom of ca. 136° and 159°. These infinite ondulating chains are linked together by phosphate tetrahedra. Each octahedron shares its vertices with two adjacent octahedra within the chain and four tetrahedra. Each tetrahedron shares three of its vertices with three octahedra that belong to two adjacent chains (Figure 5). The fourth remaining P−O bond on the phosphate tetrahedra are directed toward the center of quasi circular windows with the oxygen atoms partly as terminal OH groups or taking part in "starlike V_3 trimers" centered on vanadium V6 and V7 (Figure 5). These "V_3 trimers" consist of square planar pyramids linked together via μ_3-oxo bridge located at the center of the window. Each VO_5 from the "V_3 trimer" is linked to four tetrahedra via μ_2-oxo bridges that results in the disappearance of four OH groups.

The structure of $Cs_{\sim 5}(VO)_{10}(PO_4)_4(HPO_4)_8$ is related to that of $K_2(VO)_3(HPO_4)_4$ reported by Lii[3]. When omitting the "V_3 trimers", the negatively charged VPO framework can be

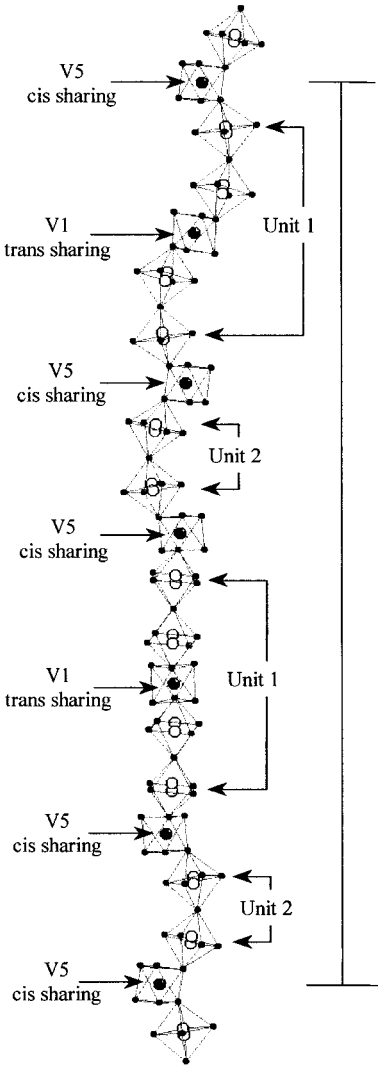

Figure 4. The chain of distorted VO_6 octahedra. Large circles are vanadium atoms, small ones are oxygen. The repeating sequence along the chain of ~58.2 Å is given on the right-hand side (vertical line).

described according to $[VO^{vv}{}_{2/2}O^{vp}{}_{4/2}]_3[HOPO^{pv}{}_{3/2}]_4$ where $O^{vv}{}_{2/2}$ means that each V-octahedron shares 2 vertices with adjacent V-octahedra, $O^{vp}{}_{4/2}$ means that each V-octahedron shares 4 vertices with P-tetrahedra and $O^{pv}{}_{3/2}$ means that each P-tetrahedron shares 3 vertices with V-octahedra. This results in the 3D macroanion $[(VO)_3(HPO_4)_4]^{u-}$ that is also present in the structure $K_2(VO)_3(HPO_4)_4$. Nevertheless, the $[(VO)_3(HPO_4)_4]^{u-}$ macroanions slightly differ for the two structures in that the chains consist only of trans sharing octahedra in $K_2(VO)_3(HPO_4)_4$ while trans and cis sharing occur in $Cs_{\sim 5}(VO)_{10}(PO_4)_4(HPO_4)_8$. The particular topology of the $[(VO)_3(HPO_4)_4]^{u-}$ macroanion in $Cs_{\sim 5}(VO)_{10}(PO_4)_4(HPO_4)_8$ generates windows large enough to accommodate supplementary vanadium atoms. These windows are covered with OH groups from the HPO_4 tetrahedra that are available to build additional vanadium polyhedra. The $[(VO)_9(HPO_4)_{12}]^{u-}$ skeleton as found in $Cs_{\sim 5}(VO)_{10}(PO_4)_4(HPO_4)_8$ can therefore include up to three supplementary vanadium atoms as four OH terminal groups change to μ_2-oxo bridges when adding one vanadium atom inside the window. Therefore, frameworks such as $[(VO)_{9+x}(PO_4)_{4x}(HPO_4)_{12-4x}]^{u-}$ $(0 \le x \le 1)$ that differ by their V/P ratios, protonation rates on the phosphates species and the overall negative charge in relation with the variable V^{4+}/V^{5+} ratios are attainable. The compound $K_2(VO)_3(HPO_4)_4$ would be the member $x = 0$ of this series with all the vanadium atoms as V^{4+} ions whereas $Cs_{\sim 5}(VO)_{10}(PO_4)_4(HPO_4)_8$ appears as the member $x = 1$ with additional V^{5+} on the VPO framework up to 20% of the total V content.

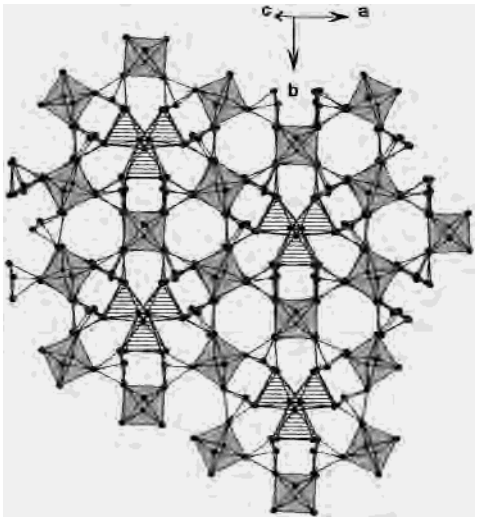

Figure 5. Partial view along the pseudo 3_2 axis: the VO_6 octahedra (grey) are part of the infinite chains, open polyhedra are PO_4 tetrahedra, the hatched polyhedra represent the V3 trimers. For sake of clarity, the metal atoms are not shown. Black circles are oxygen atoms.

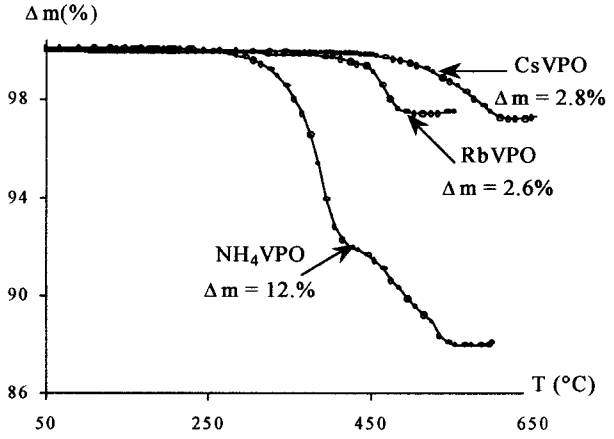

Figure 6. TG curves for the $M{\sim}5(VO)_{10}(HPO_4)_8(PO_4)_4$ compounds.

Thermogravimetric and Susceptibility Measurements. *Thermogravimetric Analyses*. Thermal analyses, using a SHIMADZU thermogravimetric analyzer, were performed on crushed samples in flowing N_2 with heating rate of 5 °C/min. After the heat treatments, the resulting products were characterized by X-ray powder diffraction analyses. Autoindexing procedure resulted in unit-cell parameters and symmetry in agreement with those reported by Lii and co-workers for the high-temperature compounds $M_2(VO)_3(P_2O_7)_2$ in the case of Cs^+ and Rb^+ compounds.[8] The decomposition products were identified as mixtures $(VO)_2P_2O_7$ and VOP_2O_6 for the ammonium compound. The $\Delta m = f(T)$ curves for the three compounds are given in Figure 6. The loss of weight (2.8% for Cs^+, 2.6% for Rb^+ and 12% for NH_4^+) compared well with the expected values for $M_{\sim 5}(VO)_{\sim 10}(PO_4)_{\sim 4}(HPO_4)_{\sim 8}$ formulas (respectively 2.85%, 3.2% and 11.8%) and was attributed to water elimination through 2 $HPO_4 \rightarrow P_2O_7 + H_2O$ condensation process with additional NH_3 elimination and $nHP_2O_7 \rightarrow nP_2O_6 + n/2H_2O$ in the case of the ammonium containing compound.

(8) Lii, K. H.; Wang, Y. P.; Wang, S. L. *J. Solid State Chem.* **1989**, *80*, 127−132.

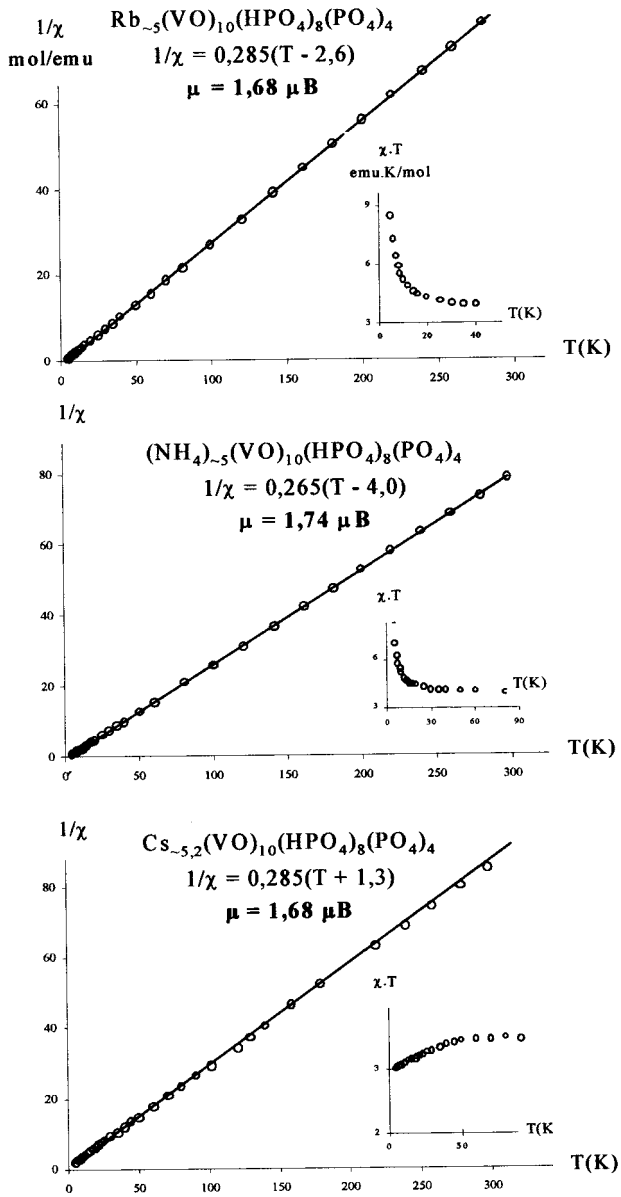

Figure 7. χT and $\chi^{-1} = f(T)$ curves. Open circles are experimental points, the full line represents the fit according to the Curie−Weiss law.

Susceptibility Measurements. Zero field cooled susceptibility measurements were conducted on 195 mg. (Cs^+), 267 mg. (Rb^+) and 197 mg. (NH_4^+) of crushed single crystals from 4.2 to 300 K in a magnetic field of 1kG using a SQUID magnetometer. After the experimental data were corrected from the diamagnetic contributions, the paramagnetic susceptibilities were fitted to the relation $\chi_M = C/(T \pm \theta)$ with the respective C values 0.285 (Cs^+), 0.285 (Rb^+) and 0.265 emu·K·mole^{-1} (NH_4^+) and calculated magnetic moments per vanadium consistent with those expected for V^{IV} ions. The $\chi T = f(T)$ and $\chi^{-1} = f(T)$ curves for the three compounds are shown in Figure 7.

Conclusion

New MVPOs have been hydrothermally isolated. The structure of $Cs_{\sim 5}(VO)_{10}(PO_4)_4(HPO_4)_8$ has been solved from X-ray crystal intensity diffraction data recorded using a CCD detector. It cristallizes in the centrosymmetric space group *C*2/*c* and is related to the structure of $K_2(VO)_3(HPO_4)_4$. The three-dimensional overall topology results from the heterocondensation of [VO_6] distorted octahedra and [VO_5] pyramids with orthophosphate units. The cæsium atoms are located inside tunnels. One of the most striking structural result described herein arises from the trans and cis sharing of the vanadium octahedra and the presence of V_3 trimers in a starlike manner. The thermogravimetric and susceptibility studies agree fairly well with the structural results. Attempts are on the way to synthesize new crystals suitable for intensity data collection for the NH_4 and Rb phases and also for the thallium compound that has been recently discovered.

Acknowledgment. The authors are indebted to Dr. T. Roisnel for the single crystal intensity data collection on the Kappa CCD diffractometer, Dr. O. Peña for susceptibility measurements, J. Le Lannic for the SEM photographs (Université de Rennes I, LCSIM, UMR 6511), and Pr. A. Riou for the single crystal intensity data collection on the CAD4 Enraf-Nonius diffractometer (Université d'Angers, IMMO, UMR 6501).

Supporting Information Available: One X-ray crystallographic file, in CIF format, and one table giving V−O−V and P−O−P bond angles are available. Access and/or ordering information is given on any current masthead page.

IC000464Y